



Published in final edited form as:

*Am J Sports Med.* 2015 September ; 43(9): 2259–2269. doi:10.1177/0363546515589165.

## Relative Strain in the Anterior Cruciate Ligament and Medial Collateral Ligament During Simulated Jump Landing and Sidestep Cutting Tasks:

### Implications for Injury Risk

**Nathaniel A. Bates, PhD<sup>\*,†,‡,§</sup>, Rebecca J. Nesbitt, PhD<sup>‡</sup>, Jason T. Shearn, PhD<sup>‡</sup>, Gregory D. Myer, PhD<sup>†,§,||,¶,#</sup>, and Timothy E. Hewett, PhD<sup>†,‡,§,||,\*\*,††,‡‡,§§,|||</sup>**

<sup>\*</sup>Department of Orthopaedic Surgery, Mayo Clinic, Rochester, Minnesota, USA.

<sup>†</sup>The Sports Health and Performance Institute, The Ohio State University, Columbus, Ohio, USA.

<sup>‡</sup>Department of Biomedical Engineering, University of Cincinnati, Cincinnati, Ohio, USA.

<sup>§</sup>Division of Sports Medicine Cincinnati Children's Hospital Medical Center, Cincinnati, Ohio, USA.

<sup>||</sup>Department of Pediatrics, College of Medicine, University of Cincinnati, Cincinnati, Ohio, USA.

<sup>¶</sup>Department of Orthopaedic Surgery, College of Medicine, University of Cincinnati, Cincinnati, Ohio, USA.

<sup>#</sup>The Micheli Center for Sports Injury Prevention, Waltham, Massachusetts, USA.

<sup>\*\*</sup>Department of Orthopaedic Surgery, Mayo Clinic, Rochester, Minnesota, USA.

<sup>††</sup>Department of Physical Medicine and Rehabilitation, Mayo Clinic, Rochester, Minnesota, USA.

<sup>‡‡</sup>Department of Physiology and Biomedical Engineering, Mayo Clinic, Rochester, Minnesota, USA.

<sup>§§</sup>Departments of Physiology and Cell Biology, Orthopaedics, Family Medicine, and Biomedical Engineering, The Ohio State University, Columbus, Ohio, USA.

### Abstract

**Background:** The medial collateral (MCL) and anterior cruciate ligaments (ACL) are, respectively, the primary and secondary ligamentous restraints against knee abduction, which is a component of the valgus collapse often associated with ACL rupture during athletic tasks. Despite this correlation in function, MCL ruptures occur concomitantly in only 20% to 40% of ACL injuries.

**Hypothesis/Purpose:** The purpose of this investigation was to determine how athletic tasks load the knee joint in a manner that could lead to ACL failure without concomitant MCL failure. It was hypothesized that (1) the ACL would provide greater overall contribution to intact knee forces

<sup>|||</sup>Address correspondence to Timothy E. Hewett, PhD, The Sports Health and Performance Institute, The Ohio State University, Columbus, Ohio, USA (timothy.hewett@osumc.edu).

One or more of the authors has declared the following potential conflict of interest

than the MCL during simulated motion tasks and (2) the ACL would show greater relative peak strain compared with the MCL during simulated motion tasks.

**Study Design:** Controlled laboratory study.

**Methods:** A 6-degrees-of-freedom robotic manipulator articulated 18 cadaveric knees through simulations of kinematics recorded from in vivo drop vertical jump and sidestep cutting tasks. Specimens were articulated in the intact-knee and isolated-ligament conditions. After simulation, each ACL and MCL was failed in uniaxial tension along its fiber orientations.

**Results:** During a drop vertical jump simulation, the ACL experienced greater peak strain than the MCL (6.1% vs 0.4%;  $P < .01$ ). The isolated ACL expressed greater peak anterior force (4.8% vs 0.3% body weight;  $P < .01$ ), medial force (1.6% vs 0.4% body weight;  $P < .01$ ), flexion torque (8.4 vs 0.4 Nm;  $P < .01$ ), abduction torque (2.6 vs 0.3 Nm;  $P < .01$ ), and adduction torque (0.5 vs 0.0 N m;  $P = .03$ ) than the isolated MCL. During failure testing, ACL specimens preferentially loaded in the anteromedial bundle failed at 637 N, while MCL failure occurred at 776 N.

**Conclusion:** During controlled physiologic athletic tasks, the ACL provides greater contributions to knee restraint than the MCL, which is generally unstrained and minimally loaded.

**Clinical Relevance:** Current findings support that multiplanar loading during athletic tasks preferentially loads the ACL over the MCL, leaving the ACL more susceptible to injury. An enhanced understanding of joint loading during in vivo tasks may provide insight that enhances the efficacy of injury prevention protocols.

## Keywords

anterior cruciate ligament injury; medial collateral ligament; cadaveric simulation; knee biomechanics; athletic tasks

---

The anterior cruciate ligament (ACL) is the primary stabilizer against anterior tibial translation and restrains up to 85% of the anterior force in the knee.<sup>8,10,39</sup> The ligament also operates as a secondary restraint against additional degrees of freedom, such as knee abduction torque.<sup>8,10,43</sup> When the ACL ruptures, these restraints are lost, resulting in joint instability. ACL failures are devastating knee injuries that have both short- and long-term implications for athletic participation and activities of daily living. Specifically, the average time for return to sport after ACL reconstruction is between 6 and 12 months, with approximately 75% of reconstructed athletes reporting negative effects on their quality of life within 15 years postoperatively.<sup>27,31,53</sup>

The current literature consistently reports that approximately 70% of ACL injuries occur during noncontact situations.<sup>7,12,35</sup> Often, noncontact ACL ruptures are preceded by one or several biomechanical factors that serve as predictors of or risk factors for the onset of injury. These factors include motions that involve rapid deceleration or change in direction,<sup>7,35</sup> increased laxity in the knee joint,<sup>42</sup> increased valgus torque at the knee,<sup>18,35,52</sup> and insufficient neuromuscular control.<sup>13,18</sup> In particular, dynamic valgus rotation has been associated with ACL injury and is a primary component used to identify ACL injury risk,<sup>18,41,48</sup> and it is also the principal knee motion restrained by the medial collateral ligament (MCL).<sup>5,18,20,38</sup> Risk factors can lead to poor control and high mechanical loads during

athletic movements like landing, cutting, and pivoting.<sup>13,34</sup> Abnormal loading can be an important mechanism for noncontact injury, especially in cutting maneuvers where knee valgus moments are most sensitive to increased loading incurred by random perturbations.<sup>33</sup> Despite these associations of knee valgus with both ACL injury risk and MCL function, less than 20% to 40% of ACL injuries have concomitant MCL injury.<sup>28,51,56</sup> Few investigators have examined the mechanisms behind this lack of dual ACL and MCL injuries.<sup>29,47,49</sup>

The objective of this study was to determine how athletic tasks load the knee joint and the ACL and MCL. To achieve this aim, robotic simulation of in vivo recorded knee kinematics on cadaveric lower extremity specimens was performed. It was hypothesized that the ACL would provide a greater overall contribution to the intact knee forces than the MCL during simulated motion tasks. It was further hypothesized that the ACL would withstand greater relative peak strain than the MCL during simulated drop landing and sidestep cutting tasks.

## METHODS

### Experimental Design

A total of 18 lower extremity human cadaveric specimens from 11 donors (mean [ $\pm$ SD] age,  $47.6 \pm 7.3$  years; mean mass,  $829 \pm 199$  N) were procured from an anatomic donations program (Anatomy Gifts Registry Inc) for inclusion in this study. As all simulation conditions in this study were applied to each test specimen, and due to the difficult nature of obtaining younger specimens who were relatively healthy at time of death, donor sex was not regulated during specimen procurement and our donor population consisted of 8 males and 3 females. These specimens were randomized into ACL ( $n = 9$ ; mean age,  $47.3 \pm 8.1$  years; mean mass,  $838 \pm 216$  N) and MCL ( $n = 9$ ; mean age,  $47.1 \pm 7.8$  years; mean mass,  $853 \pm 197$  N) study groups. Group allocation ensured that contralateral pairs were placed in opposite groups. A 6 degrees of freedom (6- DOF) robotic manipulator (KR210; KUKA Robotics Corp) with a 6-axis load cell (Theta Model; ATI Industrial Automation) mounted on the end effector articulated each limb through simulations of athletic tasks. The 6-axis load cell allowed the robotic manipulator to record both joint forces and torques along 3 perpendicular axes intersecting at the joint center point. The simulations were 6-DOF kinematics developed from in vivo 3-dimensional (3D) motion capture recordings. Explicit details of the methods of in vivo kinematic motion capture and in vitro joint simulation have previously been published in the literature and are briefly described below.<sup>4,11</sup> Motion patterns were simulated in the intact joint condition followed by an isolated ACL or MCL condition, dependent upon group randomization. In the isolated ligament conditions, the ACL or MCL was the only structure that supported load across the joint. Therefore, the isolated condition was used to quantify the individual mechanical contributions of each ligament to knee mechanics. The remaining ligament was then resected, and all simulations were repeated in a bone- only condition to quantify gravity contributions. Testing methods were reviewed and approved by the institutional review board.

### Kinematic Model

Previous literature has documented the development of a model that performs in vitro simulations of athletic movement patterns based on in vivo recordings.<sup>4</sup> Briefly, 3D motion

data were collected on a matched male (age, 24 years; height, 175 cm; mass, 68.8 kg) and female (age, 25; height, 170 cm; mass, 64.4 kg), and the joint kinematic parameters were determined.<sup>11</sup> While neither motion led to ACL injury at the time of measurement, the female subject was classified as “high risk” based on the computed peak knee abduction moment.<sup>18,40</sup> It should be noted that the subjects used in the development of this robotic simulation model are the same 2 subjects that were used to develop a validated and published finite element model of the knee.<sup>24</sup> Mathematical factors were applied to the recorded kinematics to reduce the confounding effects of skin-artifact errors and provide a 6-DOF input for in vitro simulations. Briefly, rotational kinematic values were scaled in each DOF relative to the average difference in range of motion previously observed between skin-marker and biplanar video-radiography recordings concomitantly captured on subjects who performed athletic tasks of a caliber similar to those used in the present investigation.<sup>4,39</sup> In vivo translational kinematic findings were adjusted relative to the range of translation tracked in each DOF during passive flexion of a cadaveric specimen and were unified across all specimens to reduce the confounding effects of in vivo recording inaccuracies due to skin-marker artifact error.<sup>4</sup> The mathematical factors used in the current study, along with the rationale for their selection and results of their application, have been explicitly described in previous literature.<sup>4</sup> These kinematic values were then inputted to the robotic manipulator and used to drive the simulated joint articulation (Figure 1).

### Specimen Preparation

Specimen inclusion criteria included no history of knee trauma, knee surgery, bone cancer, or ankle or shin implants. The limbs were kept frozen at  $-20^{\circ}\text{C}$  and allowed to thaw 24 hours before testing. Thawed specimens were resected of all soft tissue down to the joint capsule, leaving the collateral and cruciate ligaments and menisci intact. Anatomic landmarks were used to define the tibial joint coordinate system.<sup>15</sup> Relative to this coordinate system, custom fixtures were attached to the tibia, which was then rigidly mounted on the load cell such that the tibia, load cell, and robot end effector axes were all aligned. The tibial joint center point was digitized with a coordinate measuring machine (Faro Digitizer F04L2; FARO Technologies Inc), and all rotations, translations, forces, and torques were applied and recorded relative to this point. With the femur secured to the base, the robot was used to articulate the knee to  $45^{\circ}$ , where custom-barbed, 3-mm microminiature differential variable resistance transducers (DVRTs; LORD MicroStrain Inc) were implanted on the ACL and MCL. One DVRT was implanted on the anteromedial bundle of the ACL, slightly proximal to the tibial insertion site.<sup>6,29</sup> Three MCL implantation sites were distal to the femoral origin, at the midsubstance across the joint space, and proximal to the tibial insertion, which matches a previously described protocol.<sup>29</sup> All DVRTs were implanted parallel to the fiber alignment of their respective ligaments. A joint flexion angle of  $45^{\circ}$  was selected for DVRT implantation, as previous robotic simulations and muscle-driven flexions of the joint indicate that the ACL is unloaded around this position.<sup>50</sup> The initial limb position was different for each simulated task and was matched within  $0.5^{\circ}$  of the in vivo orientation recorded for all 3 rotational DOFs. From the initial position, limbs were incrementally loaded in compression and cycled through simulations until a peak force of 2.0 to 2.5 body weights was achieved. This compressive force matched the magnitude of vertical ground-reaction forces recorded from a single leg during drop vertical jump (DVJ)

tasks.<sup>2</sup> Similarly, a peak force of 1.5 to 2.0 body weights was achieved for sidestep cutting tasks. A more detailed account of specimen preparation and initial positioning was previously documented.<sup>4,17</sup>

### Robotic Simulation

All tests were performed at room temperature, and the joint was consistently hydrated with saline. Irrespective of specimen sex, movement patterns from all 4 athletic tasks (male DVJ, male sidestep cut, female DVJ, and female sidestep cut) were performed on each limb in a randomized order (Figure 2). Before each simulation, the specimen was cycled 10 times to precondition the joint and minimize viscoelastic effects. Preconditioning was followed by a second set of 10 cycles during which knee forces, knee torques, and ligament strains were recorded. After each motion was completed, the specimen was manually articulated to the initial position for the next simulated task and the process was repeated. Once all simulations were run in the intact condition, the specimen was resected of all soft tissues along with the distal portions of the femoral condyles to achieve the isolated ACL or isolated MCL condition, dependent on specimen grouping (Figure 3). In this isolated condition, the remaining ligament was the only structure transmitting force across the joint, which allowed for quantification of its respective contributions to force resistance during motion. All simulations were repeated in the isolated condition. After simulation, the joint was returned to initial contact orientation, compressed to an unloaded position, and slowly distracted to identify the neutral strain position of the ligament. With the isolated ligament as the only intact load-bearing structure, neutral strain was identified when the force sensors first registered a constant distraction force. The remaining ligament was then resected, and all simulations were repeated in a bone-only condition to quantify gravity contributions.

### Uniaxial Failure Loading

After the completion of all robotic simulations for each specimen, the full ACL and MCL were removed in a bone-ligament-bone format. With DVRTs removed, these specimens were individually secured into mechanical fixtures with bone cement and affixed to a uniaxial servohydraulic testing machine (Model 8501; Instron) with a 10-kN load cell. Each specimen was oriented such that the ligament fibers were aligned with the loading axis of the Instron. ACL specimens were oriented such that the anteromedial bundle was preferentially loaded, as DVRTs were implanted on this bundle during robotic simulation. Before failure testing, a small preload of 4 N was applied to each specimen, after which the specimens were cyclically preconditioned between 0% and 3% strain with a cycling rate of 1 Hz over 50 cycles. During failure testing, the specimens were loaded linearly at a strain rate of 20% per second until failure was achieved, which corresponds with previous investigations.<sup>1,23,54</sup> Ligament length was measured with calipers while the specimen was in the neutral strain position. Displacements recorded by the testing machine were compared with this neutral strain length to monitor the noted rate of strain change and strain limits during uniaxial failure testing.

### Data Analysis

All forces and torques were analyzed in the tibial reference frame based on the knee joint coordinate system.<sup>15</sup> The forces and torques recorded during the bone-only condition

represent values generated from gravity and robot inertia; therefore, they were subtracted from the corresponding intact and isolated-ligament conditions. All forces and torques were filtered by use of a Fourier transform with a 12-Hz frequency to remove noise. Translational forces were normalized to percentage of body weight. The identification of a neutral strain position, where the ligament exhibited neither strain nor slack, allowed for the calculation of absolute ligament strain rather than strain relative to the insertion orientation of the DVRT. The eighth and ninth cycles of each 10-cycle set were used for data analysis to eliminate cycle effects. All data were normalized to percentage of landing cycle, which began at the point of initial contact and ended when the minimum center of gravity was achieved. Univariate analysis of variance (ANOVA) was used to evaluate statistical significance ( $\alpha < .05$ ) between ligaments (ACL vs MCL) during each condition. Statistical analyses were performed in MATLAB (v 2012b; The MathWorks Inc) by use of built-in functions and verified in SPSS (v 21; IBM Corp).

## RESULTS

### Ligament Strain

For the intact knee, the strain exhibited by the ACL throughout all simulated tasks was consistently greater than the strain exhibited by the MCL (Figure 4). For both ligaments, strains were greater throughout the intact knee simulations than during isolated ligament simulations. The mean strain of the ACL-intact versus ACL-isolated knee throughout each motion task ( $\pm$ SD) was  $4.3\% \pm 0.5\%$  versus  $1.5\% \pm 2.1\%$  for female DVJ,  $3.4\% \pm 0.2\%$  versus  $1.0\% \pm 2.5\%$  for male DVJ,  $2.1\% \pm 0.9\%$  versus  $0.7\% \pm 1.0\%$  for female sidestep cut, and  $4.6\% \pm 1.0\%$  versus  $3.3\% \pm 1.8\%$  for male sidestep cut; however, none of these differences were statistically significant ( $P > .31$ ). Relative to ligament length at the neutral strain position, the ACL was generally more extended throughout the duration of each simulated task, while the MCL was generally more contracted. For the isolated ligament condition, the MCL was unstrained (strain  $< 0.0\%$ ) for all simulated tasks. During the intact-knee simulation for female DVJ, the average peak ACL strain ( $6.1\%$ ) was greater than the average peak MCL strain ( $0.7\%$ ;  $P = .01$ ) (Figure 5). This was also true for the intact-knee female cut ( $3.8\%$  vs  $-0.3\%$ ;  $P = .03$ ), male DVJ ( $6.1\%$  vs  $0.1\%$ ;  $P = .01$ ), and male cut ( $7.0\%$  vs  $1.2\%$ ;  $P = .01$ ) as well as for the isolated-ligament-knee male cut ( $6.3\%$  vs  $-0.6\%$ ;  $P = .04$ ).

### Ligament Loading

During both male and female simulated DVJs, the ACL exhibited greater peak anterior and medial force than the MCL ( $P = .01$ ) (Table 1). In both sexes, the ACL also expressed greater peak flexion, abduction, and adduction torques ( $P < .05$ ) during simulated DVJs. Neither the ACL nor the MCL expressed significant forces (peak  $< 0.5\%$  X body weight) in the posterior, lateral, or compression DOFs for either DVJ model. Similarly, neither ligament exhibited significant torques (peak  $< 0.5$  N m) in the external, internal, or adduction DOFs. For both the translational and rotational loading components, the ACL exhibited greater contributions than the MCL (Figures 6 and 7).

Fewer statistically significant differences were found between the ACL and MCL during sidestep cut simulations than during DVJ simulations (Table 2). Both the male and female sidestep cut models exhibited greater magnitudes of extension torque in the ACL than in the MCL ( $P < .05$ ). The male sidestep cut model also exhibited greater peak loads in the ACL than the MCL for anterior force ( $P > .01$ ), flexion torque ( $P > .01$ ), and abduction torque ( $P > .01$ ). These differences were not present in the female sidestep cut simulations. Neither the ACL nor MCL exhibited clinically relevant peak magnitudes of posterior force, lateral force, compressive force, external torque, and internal torque during sidestep cut simulations.

### Uniaxial Failure

During uniaxial failure testing, there were no statistically significant differences ( $P > .05$ ) in ultimate load at failure between the ACL ( $637 \pm 135$  N;  $79.2\% \pm 0.3\%$  body weight) and MCL ( $776 \pm 291$  N;  $94.8\% \pm 0.4\%$  body weight).

## DISCUSSION

The purpose of the present study was to use methods of robotic simulation to determine how athletic tasks load the knee joint and the ACL and MCL. It was hypothesized and confirmed by the data that the ACL would make larger mechanical contributions to knee joint restraint during athletic tasks than the MCL. Data from the current investigation correlate well with biomechanical outcomes from impact-driven, in vitro simulations of ACL injury which demonstrated that the ACL is disproportionately loaded compared with the MCL during a landing activity.<sup>49</sup>

Specifically, the hypothesis that the ACL would have a greater overall contribution to intact knee forces than the MCL during simulated motion tasks was supported. Data from the present study showed that irrespective of sex, DVJ and sidestep cutting tasks generated significantly greater peak loads in the ACL than in the MCL. This indicates that the ACL contributed more to knee restraint than the MCL during physiologic athletic tasks. Previous literature from impact simulations confirmed the continued presence of a bias in the ratio of ACL:MCL loading during injury scenarios that incorporated knee abduction torques.<sup>49</sup> The biomechanical disparity in knee ligament loading ratios, reported in the current investigation and previous literature, could potentially explain why only 20% to 40% of ACL injuries experience concomitant MCL rupture.<sup>28,51</sup>

The hypothesis that the ACL would undergo greater relative peak strain than the MCL during simulated DVJ and sidestep cutting tasks was also supported. The current investigation found that regardless of sex, during the simulation of athletic tasks in the intact knee, the ACL was continuously subjected to greater strain than the MCL. This is in agreement with previous investigations reporting that ACL to MCL strain ratios exceed 1.7 during simulated ground impact.<sup>49</sup> In the present study, the ACL to MCL strain ratios exhibited even greater disparity as the mean ratio for DVJ simulations was 15.3 and for sidestep cut simulations was 10.8. The increased ratios in the present study were the result of minimal strain being observed on the MCL throughout each simulation. In previous literature, loads were generated through an impulse force applied to the foot.<sup>49</sup> For the specified investigation, specimen position was passively constrained through the ligaments

within the joint as well as a series of cables that were attached to tendons surrounding the joint and tensioned to a constant force. Computational models demonstrate that muscle force activations are in flux throughout in vivo landing, constantly adjusting to actively restrain the knee.<sup>21</sup> In the present study, specimen position was confined to the predetermined path generated from in vivo recorded kinematics. These differences in testing method could have led to the magnitude differences observed in ACL to MCL strain ratios. Further, the impact system was designed to generate ACL rupture,<sup>49</sup> whereas the current system reproduced motions that were not damaging to the limbs as was documented previously.<sup>4</sup> ACL injuries are often attributed to poor neuromuscular control, which results in abnormal loading of passive knee restraints.<sup>7,13,18</sup> Therefore, it would be expected that ACL to MCL strain ratios would decrease during impact simulations, as they represent a loss of neuromuscular control and invoke passive structures like the MCL to constrain the knee. Conversely, the in vivo motions emulated by robotic simulation were representative of tasks that exhibited greater control through neuromuscular pathways. These conditions minimized mechanical demand on passive knee structures, which led to large ACL to MCL strain ratios as the MCL strain approached 0.0%.

Data from the present study regarding ligamentous contributions to knee restraint correspond with previous findings.<sup>3,29</sup> In the present study, the ACL contributed significant torque (>1.0 N m) to the flexion and abduction DOFs but did not contribute significantly to internal torque resistance. Significant evidence, including several biomechanical testing mechanisms, has supported valgus collapse as a primary mechanism of noncontact ACL injury.<sup>18,25,26,46,49</sup> Yet some investigators attribute ACL injury to increased internal tibial torsion.<sup>37,44,45</sup> Along with previous data that demonstrated ACL strain values increased more from knee abduction rotations than from internal tibial rotation,<sup>3,29</sup> force contributions from the DVJ and sidestep cut tasks simulated in the current study indicated that during athletic task performance, the ACL may be more susceptible to abduction torques than internal tibial torques.

In the present simulation model, the ACL made significant contributions (force >1.0% body weight) to the anterior and medial forces. This corresponds with previous literature that identifies the ACL as a primary resistor to anterior tibial translation and a secondary resistor to medial tibial translation.<sup>8,10,14,43</sup> The fact that the ACL followed accepted mechanical conventions of force resistance adds validity to the novel simulation method used in this investigation.

As documented in the literature, simulations in the current study generated between 1.5 and 2.5 body weights of compressive force at the knee in each specimen.<sup>4</sup> This compressive load corresponded with the increase in total knee force beginning at approximately 20% of the landing phase. The compressive force was protective to the ACL as it unloaded the ligament by 20% of landing phase and ACL loads did not reemerge until after 50% of landing phase, when peak compression had subsided. This finding conflicts with other reports that have indicated tibiofemoral compression drives the femoral condyles along the slope of the tibial plateau to create anterior tibial translation and increase ACL strain.<sup>32,36-38</sup> However, those studies invoked average loads of 4.4 to 6.0 kN that were 2 to 4 times the magnitude of compressive loads in the current study, which may be responsible for the anterior shift of the



tibia. In the current study, the calculated kinematics did not exhibit an anterior shift during the landing phase.

ACL failure load in the present study was lower than in previous reports. The previously reported failure load of the ACL in specimens of 40- to 50-year-old donors was between 1160 and 1503 N depending upon loading orientation.<sup>54</sup> This is between 182.1% and 235.9% greater than the present data. However, as noted by the 343-N change in the prior investigation,<sup>54</sup> slight changes in specimen orientation can drastically influence the peak load to failure during mechanical testing. In the present tests, specimens were preferentially loaded in the anteromedial bundle as that bundle was monitored by DVRTs during robotic simulation. The preferential loading was further appropriate because ACL injuries typically occur within 50 milliseconds of initial contact in less than 30° of knee flexion and the anteromedial bundle has been shown to be significantly more responsive to external load than the posterolateral bundle in this relatively extended knee position.<sup>7,22,26</sup> As such, the anteromedial bundle would likely absorb the majority of abnormal loading in a relatively extended position and would be more likely to serve as the point of failure in such an orientation. Previous methods of ACL failure applied tensioning in line with the ligament fiber orientation or along the tibial axis of a vertically oriented ligament.<sup>54</sup> Ideally, these alignments would have maximized the fibril contributions and cross-sectional area that resisted loading. Methods applied in the current investigation likely limited fibril resistance and cross-sectional area primarily to the anteromedial bundle; therefore, the lower failure loads were unsurprising.

In the current model, all soft tissue outside the joint capsule were removed from the cadaveric specimens. This practice is common in kinematically defined robotic simulations as the robotic manipulator drives the bony structures to their predesignated positions and, therefore, replaces the functional role of the musculature.<sup>9,16,17,19,43</sup> Some kinematically defined robotic simulations have left intact the soft tissues immediately surrounding the joint, such as hamstrings and quadriceps tendons.<sup>3,30,55</sup> This allows for the application of loads outside of recorded kinematics and could be used to simulate musculature imbalances and other conditions. For example, tension applied to the quadriceps tendon during a robotically simulated Lachman test has been shown to increase the magnitude of both internal tibial rotation and knee valgus rotation.<sup>3,30,55</sup> Future investigations with the present model could apply these concepts of a combined positional and force-torque control to examine the effect of conditions such as quadriceps-dominant muscle activations or strengthening through neuromuscular intervention training on knee mechanics during simulated athletic tasks. The relative balance of muscle activation ratios in the current subjects was unknown.

A limitation of this study was that the individual contributions of the ACL and MCL to overall knee biomechanics were determined relative to the isolated ligament condition, where all additional intra-articular structures of the knee were resected. When specimens transitioned from the intact to isolated ligament condition, the magnitude of strain in the ACL and MCL decreased. The mean shift experienced across each simulated task averaged between 1.3% and 2.8% strain in the ACL. While the strain decrease was observed in the MCL as well, it was largely inconsequential as the ligament was already mostly unstrained

throughout the majority of simulated tasks. This decline in strain magnitude indicated that ligament slack increased and load decreased as additional knee structures were resected. Therefore, interaction between the ACL and MCL and additional intra-articular knee structures likely influences the respective biomechanics of both ligaments. For this reason, comparison of the ACL-deficient or MCL-deficient knee mechanics to intact knee mechanics may provide a more precise depiction of the individual contributions from each ligament to intact knee restraint. Unfortunately, as all internal knee structures were resected simultaneously, the primary contributors to this strain slackening remained indeterminable.

Another limitation is that the input kinematic values in the present model were derived from a single male and single female subject. While average kinematic values calculated from a subject cohort may have been more representative of the population mean, the calculation of average kinematics can wash out physiologic occurrences of natural motion. This washout is due to the waveform variability that is associated with various DOFs during optical motion analysis.<sup>11</sup> Further, the merging of individual datasets that represent functional joint motion into a population average may create kinematic inputs that are physiologically unsustainable in the cadaveric joint. For these reasons, the current model was developed from individual kinematics. As mentioned, the subjects in this investigation were also used in the development of a validated finite element model of the knee.<sup>24</sup> Further study is necessary to determine whether population average kinematic results are sustainable in a cadaveric knee and, if so, how those mechanical outcomes compare with the presently reported data.

## CONCLUSION

Data from this investigation demonstrate the relative and differential contributions of the ACL and MCL to knee joint restraint during simulated in vivo athletic tasks. In these controlled athletic tasks, where no damage was inflicted on the specimen, the ACL exhibited significantly greater loading and strain than the MCL. In most of the simulated conditions, the MCL remained unstrained.

## ACKNOWLEDGMENT

The authors acknowledge the support of the staff at the Sports Health and Performance Institute at The Ohio State University and the Sports Medicine Biodynamics Laboratory at Cincinnati Children's Hospital.

source of funding: This work was supported by the National Institutes of Health/NIAMS (Grants R01-AR049735, R01-AR055563, R01-AR056660, and R01-AR056259).

## REFERENCES

1. Arnout N, Myncke J, Vanlauwe J, Labey L, Lismont D, Bellemans J. The influence of freezing on the tensile strength of tendon grafts: a biomechanical study. *Acta Orthop Belg.* 2013;79(4):435–443. [PubMed: 24205775]
2. Bates NA, Ford KR, Myer GD, Hewett TE. Impact differences in ground reaction force and center of mass between the first and second landing phases of a drop vertical jump and their implications for injury risk assessment. *J Biomech.* 2013;46(7):1237–1241. [PubMed: 23538000]
3. Bates NA, Myer GD, Shearn JT, Hewett TE. Anterior cruciate ligament biomechanics during robotic and mechanical simulations of physiologic and clinical motion tasks: a systematic review and meta-analysis. *Clin Biomech.* 2015;30(1):1–13.

4. Bates NA, Nesbitt RJ, Shearn JT, Myer GD, Hewett TE. A novel methodology for the simulation of athletic tasks on cadaveric knee joints with respect to in vivo kinematics [published online April 14, 2015]. *Ann Biomed Eng*. doi:10.1007/s10439-015-1285-8.
5. Battaglia MJ II, Lenhoff MW, Ehteshami JR, et al. Medial collateral ligament injuries and subsequent load on the anterior cruciate ligament: a biomechanical evaluation in a cadaveric model. *Am J Sports Med*. 2009;37(2):305–311. [PubMed: 19098154]
6. Beynnon B, Howe JG, Pope MH, Johnson RJ, Fleming BC. The measurement of anterior cruciate ligament strain in vivo. *Int Orthop*. 1992;16(1):1–12. [PubMed: 1572761]
7. Boden BP, Dean GS, Feagin JA, Garrett WE. Mechanisms of anterior cruciate ligament injury. *Orthopedics*. 2000;23(6):573–578. [PubMed: 10875418]
8. Boguszewski DV. Characterizing the Porcine Knee as a Biomechanical Surrogate Model of the Human Knee to Study the Anterior Cruciate Ligament [PhD dissertation]. Cincinnati, OH: Biomedical Engineering, University of Cincinnati; 2012.
9. Boguszewski DV, Shearn JT, Wagner CT, Butler DL. Investigating the effects of anterior tibial translation on anterior knee force in the porcine model: is the porcine knee ACL dependent? *J Orthop Res*. 2011;29(5):641–646. [PubMed: 21437942]
10. Butler DL, Noyes FR, Grood ES. Ligamentous restraints to anteriorposterior drawer in the human knee: a biomechanical study. *J Bone Joint Surg Am*. 1980;62(2):259–270. [PubMed: 7358757]
11. Ford KR, Myer GD, Hewett TE. Reliability of landing 3D motion analysis: implications for longitudinal analyses. *Med Sci Sports Exerc*. 2007;39(11):2021–2028. [PubMed: 17986911]
12. Gianotti SM, Marshall SW, Hume PA, Bunt L. Incidence of anterior cruciate ligament injury and other knee ligament injuries: a national population-based study. *J Sci Med Sport*. 2009;12(6):622–627. [PubMed: 18835221]
13. Griffin LY, Agel J, Albohm MJ, et al. Noncontact anterior cruciate ligament injuries: risk factors and prevention strategies. *J Am Acad Orthop Surg*. 2000;8(3):141–150. [PubMed: 10874221]
14. Grood ES, Noyes FR, Butler DL, Suntay WJ. Ligamentous and capsular restraints preventing straight medial and lateral laxity in intact human cadaver knees. *J Bone Joint Surg Am*. 1981;63(8):1257–1269. [PubMed: 7287796]
15. Grood ES, Suntay WJ. A joint coordinate system for the clinical description of three-dimensional motions: application to the knee. *J Biomech Eng*. 1983;105(2):136–144. [PubMed: 6865355]
16. Herfat ST, Boguszewski DV, Nesbitt RJ, Shearn JT. Effect of perturbing a simulated motion on knee and anterior cruciate ligament kinetics. *J Biomech Eng*. 2012;134(10):104504.
17. Herfat ST, Boguszewski DV, Shearn JT. Applying simulated in vivo motions to measure human knee and ACL kinetics. *Ann Biomed Eng*. 2012;40(7):1545–1553. [PubMed: 22227973]
18. Hewett TE, Myer GD, Ford KR, et al. Biomechanical measures of neuromuscular control and valgus loading of the knee predict anterior cruciate ligament injury risk in female athletes: a prospective study. *Am J Sports Med*. 2005;33(4):492–501. [PubMed: 15722287]
19. Howard RA, Rosvold JM, Darcy SP, et al. Reproduction of in vivo motion using a parallel robot. *J Biomech Eng*. 2007;129(5):743–749. [PubMed: 17887900]
20. Hull ML, Berns GS, Varma H, Patterson HA. Strain in the medial collateral ligament of the human knee under single and combined loads. *J Biomech*. 1996;29(2):199–206. [PubMed: 8849813]
21. Kar J, Quesada PM. A numerical simulation approach to studying anterior cruciate ligament strains and internal forces among young recreational women performing valgus inducing stop-jump activities. *Ann Biomed Eng*. 2012;40(8):1679–1691. [PubMed: 22527014]
22. Kato Y, Ingham SJ, Maeyama A, et al. Biomechanics of the human triplebundle anterior cruciate ligament. *Arthroscopy*. 2012;28(2):247–254. [PubMed: 22019233]
23. Kennedy JC, Hawkins RJ, Willis RB, Danylchuk KD. Tension studies of human knee ligaments: yield point, ultimate failure, and disruption of the cruciate and tibial collateral ligaments. *J Bone Joint Surg Am*. 1976;58(3):350–355. [PubMed: 1262366]
24. Kiapour A, Kiapour AM, Kaul V, et al. Finite element model of the knee for investigation of injury mechanisms: development and validation. *J Biomech Eng*. 2014;136(1):011002.
25. Koga H, Nakamae A, Shima Y, et al. Mechanisms for noncontact anterior cruciate ligament injuries: knee joint kinematics in 10 injury situations from female team handball and basketball. *Am J Sports Med*. 2010;38(11):2218–2225. [PubMed: 20595545]

26. Krosshaug T, Nakamae A, Boden BP, et al. Mechanisms of anterior cruciate ligament injury in basketball: video analysis of 39 cases. *Am J Sports Med.* 2007;35(3):359–367. [PubMed: 17092928]
27. Kvist J Rehabilitation following anterior cruciate ligament injury: current recommendations for sports participation. *Sports Med.* 2004;34(4):269–280. [PubMed: 15049718]
28. LaPrade RF, Wentorf FA, Fritts H, Gundry C, Hightower CD. A prospective magnetic resonance imaging study of the incidence of posterolateral and multiple ligament injuries in acute knee injuries presenting with a hemarthrosis. *Arthroscopy.* 2007;23(12):1341–1347. [PubMed: 18063179]
29. Levine JW, Kiapour AM, Quatman CE, et al. Clinically relevant injury patterns after an anterior cruciate ligament injury provide insight into injury mechanisms. *Am J Sports Med.* 2013;41(2):385–395. [PubMed: 23144366]
30. Li G, Papannagari R, DeFrate LE, Yoo JD, Park SE, Gill TJ. The effects of ACL deficiency on mediolateral translation and varus-valgus rotation. *Acta Orthop.* 2007;78(3):355–360. [PubMed: 17611849]
31. Lohmander LS, Ostenberg A, Englund M, Roos H. High prevalence of knee osteoarthritis, pain, and functional limitations in female soccer players twelve years after anterior cruciate ligament injury. *Arthritis Rheum.* 2004;50(10):3145–3152. [PubMed: 15476248]
32. Markolf KL, Jackson SR, Foster B, McAllister DR. ACL forces and knee kinematics produced by axial tibial compression during a passive flexion-extension cycle. *J Orthop Res.* 2014;32(1):89–95. [PubMed: 23996893]
33. McLean SG, Huang X, Su A, van den Bogert AJ. Sagittal plane biomechanics cannot injure the ACL during sidestep cutting. *Clin Biomech.* 2004;19:828–838.
34. McLean SG, Huang X, van den Bogert AJ. Association between lower extremity posture at contact and peak knee valgus moment during sidestepping: implications for ACL injury. *Clin Biomech.* 2005;20(8):863–870.
35. McNair PJ, Marshall RN, Matheson JA. Important features associated with acute anterior cruciate ligament injury. *N Z Med J.* 1990;103(901):537–539. [PubMed: 2243642]
36. Meyer EG, Baumer TG, Slade JM, Smith WE, Haut RC. Tibiofemoral contact pressures and osteochondral microtrauma during anterior cruciate ligament rupture due to excessive compressive loading and internal torque of the human knee. *Am J Sports Med.* 2008;36(10):1966–1977. [PubMed: 18490469]
37. Meyer EG, Haut RC. Anterior cruciate ligament injury induced by internal tibial torsion or tibiofemoral compression. *J Biomech.* 2008;41(16):3377–3383. [PubMed: 19007932]
38. Meyer EG, Haut RC. Excessive compression of the human tibio-femoral joint causes ACL rupture. *J Biomech.* 2005;38(11):2311–2316. [PubMed: 16154419]
39. Miranda DL, Rainbow MJ, Crisco JJ, Fleming BC. Kinematic differences between optical motion capture and biplanar videoradiography during a jump-cut maneuver. *J Biomech.* 2013;46(3):567–573. [PubMed: 23084785]
40. Myer GD, Ford KR, Brent JL, Hewett TE. Differential neuromuscular training effects on ACL injury risk factors in “high-risk” versus “low-risk” athletes. *BMC Musculoskelet Disord.* 2007;8(39):1–7. [PubMed: 17204151]
41. Myer GD, Ford KR, Khoury J, Succop P, Hewett TE. Biomechanics laboratory-based prediction algorithm to identify female athletes with high knee loads that increase risk of ACL injury. *Br J Sports Med.* 2011;45(4):245–252. [PubMed: 20558526]
42. Myer GD, Ford KR, Paterno MV, Nick TG, Hewett TE. The effects of generalized joint laxity on risk of anterior cruciate ligament injury in young female athletes. *Am J Sports Med.* 2008;36(6):1073–1080. [PubMed: 18326833]
43. Nesbitt RJ, Herfat ST, Boguszewski DV, Engel AJ, Galloway MT, Shearn JT. Primary and secondary restraints of human and ovine knees for simulated in vivo gait kinematics. *J Biomech.* 2013;47(9):2022–2027. [PubMed: 24326097]
44. Oh YK, Kreinbrink JL, Wojtys EM, Ashton-Miller JA. Effect of axial tibial torque direction on ACL relative strain and strain rate in an in vitro simulated pivot landing. *J Orthop Res.* 2012;30(4):528–534. [PubMed: 22025178]

45. Oh YK, Lipps DB, Ashton-Miller JA, Wojtys EM. What strains the anterior cruciate ligament during a pivot landing? *Am J Sports Med.* 2012;40(3):574–583. [PubMed: 22223717]
46. Olsen OE, Myklebust G, Engebretsen L, Bahr R. Injury mechanisms for anterior cruciate ligament injuries in team handball: a systematic video analysis. *Am J Sports Med.* 2004;32(4):1002–1012. [PubMed: 15150050]
47. Pressman A, Johnson DH. A review of ski injuries resulting in combined injury to the anterior cruciate ligament and medial collateral ligaments. *Arthroscopy.* 2003;19(2):194–202. [PubMed: 12579153]
48. Quatman CE, Hewett TE. The anterior cruciate ligament injury controversy: is “valgus collapse” a sex-specific mechanism? *Br J Sports Med.* 2009;43(5):328–335. [PubMed: 19372087]
49. Quatman CE, Kiapour AM, Demetropoulos CK, et al. Preferential loading of the ACL compared with the MCL during landing: a novel in sim approach yields the multiplanar mechanism of dynamic valgus during ACL injuries. *Am J Sports Med.* 2014;42(1):177–186. [PubMed: 24124198]
50. Renstrom P, Arms SW, Stanwyck TS, Johnson RJ, Pope MH. Strain within the anterior cruciate ligament during hamstring and quadriceps activity. *Am J Sports Med.* 1986;14(1):83–87. [PubMed: 3752352]
51. Sankar WN, Wells L, Sennett BJ, Wiesel BB, Ganley TJ. Combined anterior cruciate ligament and medial collateral ligament injuries in adolescents. *J Pediatr Orthop.* 2006;26(6):733–736. [PubMed: 17065935]
52. Shin CS, Chaudhari AM, Andriacchi TP. The effect of isolated valgus moments on ACL strain during single-leg landing: a simulation study. *J Biomech.* 2008;42(3):280–285. [PubMed: 19100550]
53. von Porat A, Roos EM, Roos H. High prevalence of osteoarthritis 14 years after an anterior cruciate ligament tear in male soccer players: a study of radiographic and patient relevant outcomes. *Ann Rheum Dis.* 2004;63(3):269–273. [PubMed: 14962961]
54. Woo SL, Hollis JM, Adams DJ, Lyon RM, Takai S. Tensile properties of the human femur-anterior cruciate ligament-tibia complex: the effects of specimen age and orientation. *Am J Sport Med.* 1991;19(3):217–227.
55. Yoo JD. The effect of anterior cruciate ligament reconstruction on knee joint kinematics under simulated muscle loads. *Am J Sports Med.* 2005;33(2):240–246. [PubMed: 15701610]
56. Yoon KH, Yoo JH, Kim KI. Bone contusion and associated meniscal and medial collateral ligament injury in patients with anterior cruciate ligament rupture. *J Bone Joint Surg Am.* 2011;93(16):1510–1518. [PubMed: 22204006]

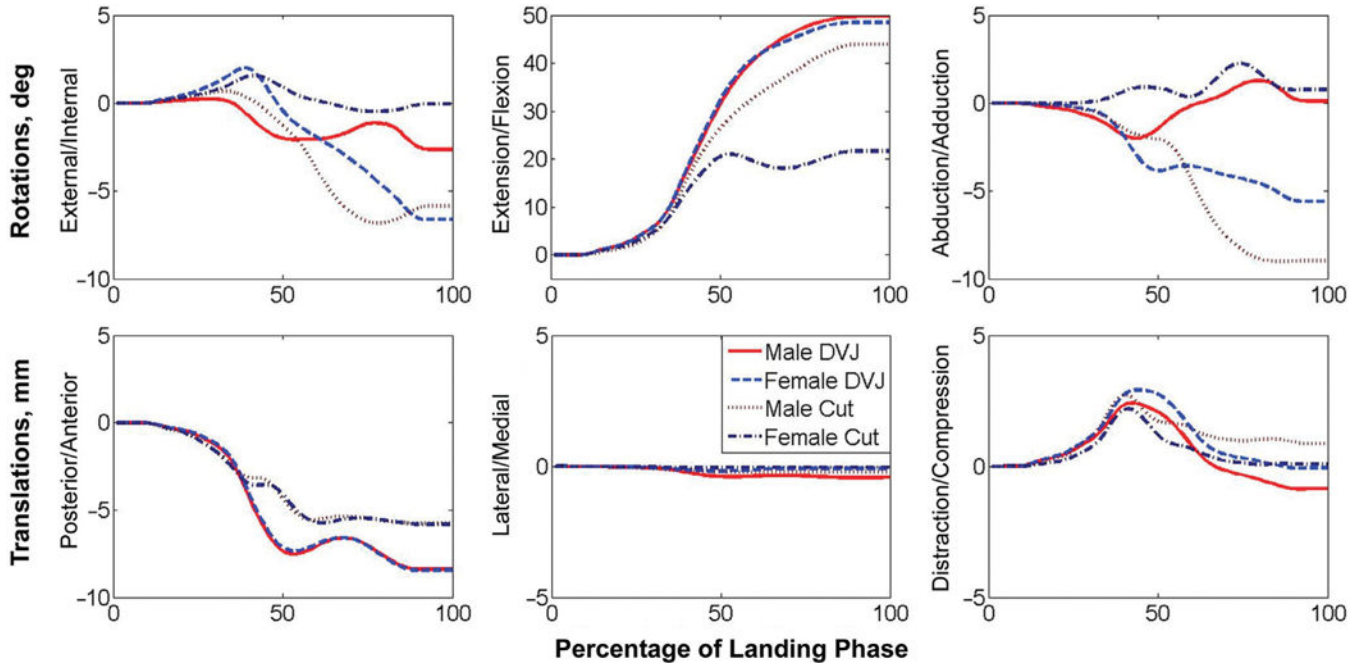


**Figure 1.** Kinematic pathways for all 6 degrees of freedom for each of the 4 motions simulated. Curves represent the kinematic changes that the joint underwent from its original orientation (in vivo recorded position at initial contact) through the end of the landing phase of motion (in vivo recorded position where minimum center of gravity was achieved). For each cycle of simulation, once 100% landing phase was reached, the limb was articulated back to its starting orientation through the reverse kinematic pathway before the following cycle of motion was initiated.

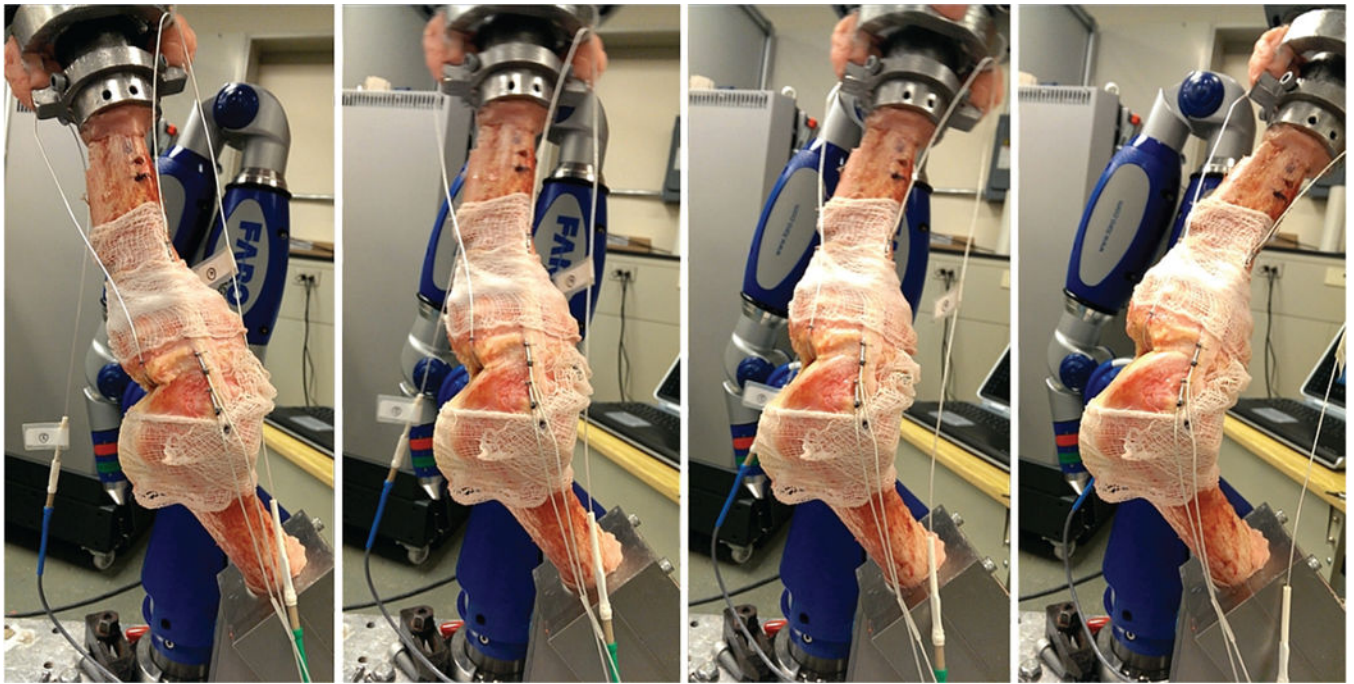


**Figure 2.** Sagittal view of a lower extremity specimen affixed to the robot manipulator and articulated through a male drop vertical jump. Moving from left to right, each frame depicts knee position at initial contact to begin each cycle, at 2 separate points in midflexion, and at the peak flexion angle reached in each cycle during simulation. Simulations for the selected athletic tasks are cycled through the landing phase, which is represented by the period from initial contact to maximum knee flexion as stated in previous literature.<sup>2,4</sup>

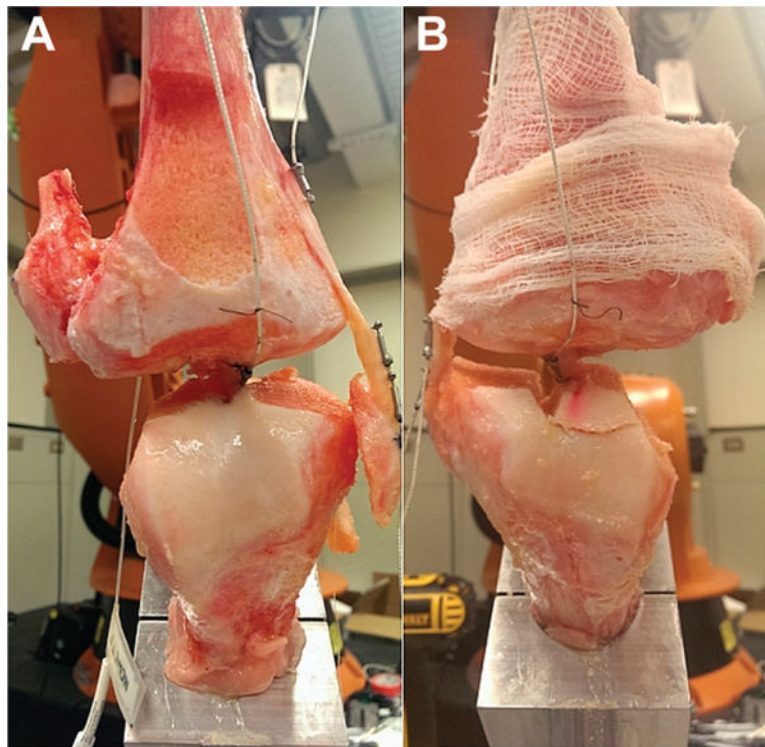


**Figure 3.** Frontal plane view of a specimen in the (A) anterior cruciate ligament (ACL)-isolated condition and the (B) medial collateral ligament (MCL)-isolated condition. While the ACL may appear intact for the MCL-isolated condition, its femoral insertion was severed from the bone and bore no mechanical load.



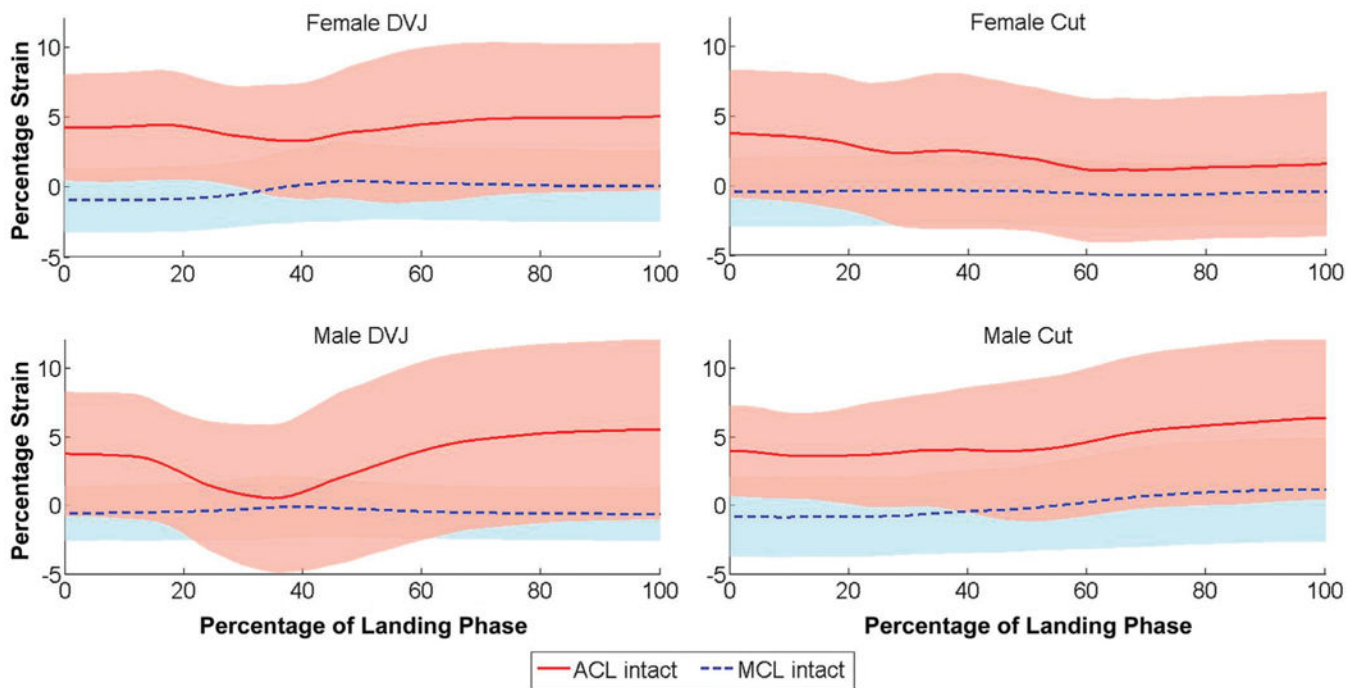


**Figure 4.**

Population mean absolute strains for the anterior cruciate ligament (ACL) and medial collateral ligament (MCL) throughout each simulated motion task. Throughout the majority of simulated tasks, the MCL average was unstrained, while the ACL average expressed up to 6.3% strain. DVJ, drop vertical jump.

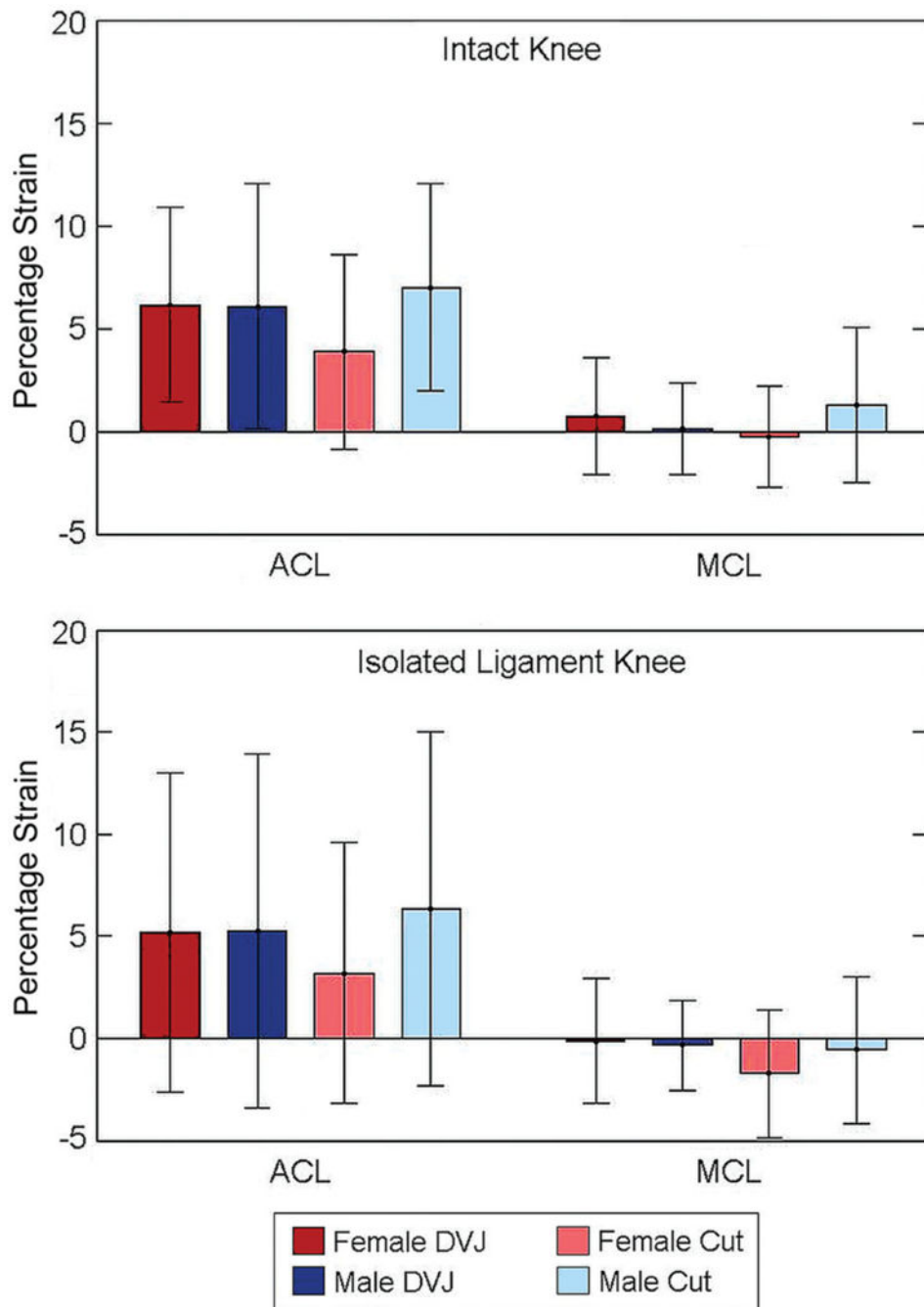


**Figure 5.** Average peak anterior cruciate ligament (ACL) and medial collateral ligament (MCL) strains for the specimen population during each simulated task. DVJ, drop vertical jump.

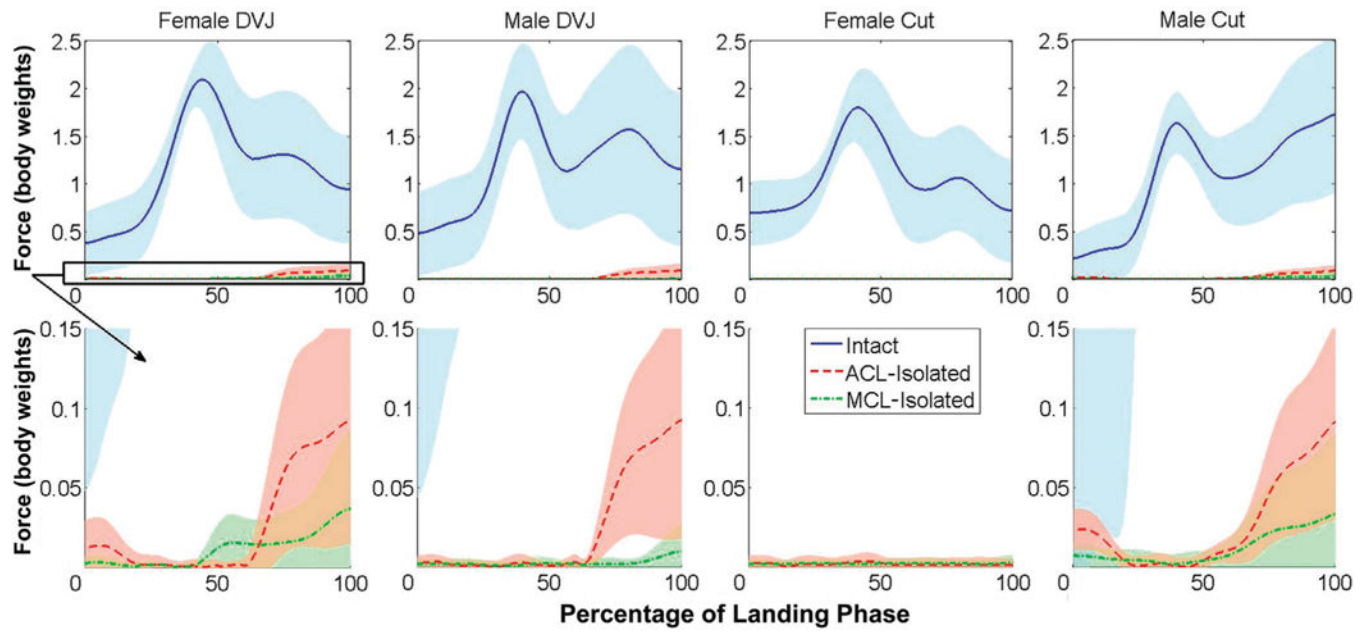


**Figure 6.**

Total knee force during landing phase of athletic tasks. Sum of the average translational components during each simulated task for the intact knee, anterior cruciate ligament (ACL)–isolated knee, and medial collateral ligament (MCL)–isolated knee. As noted in previous simulations of the stance phase of gait,<sup>43</sup> the ACL and MCL offer limited contributions to joint restraint when compared with the total joint force. In 3 of 4 simulated tasks, the ACL had greater overall mechanical contributions than the MCL. DVJ, drop vertical jump

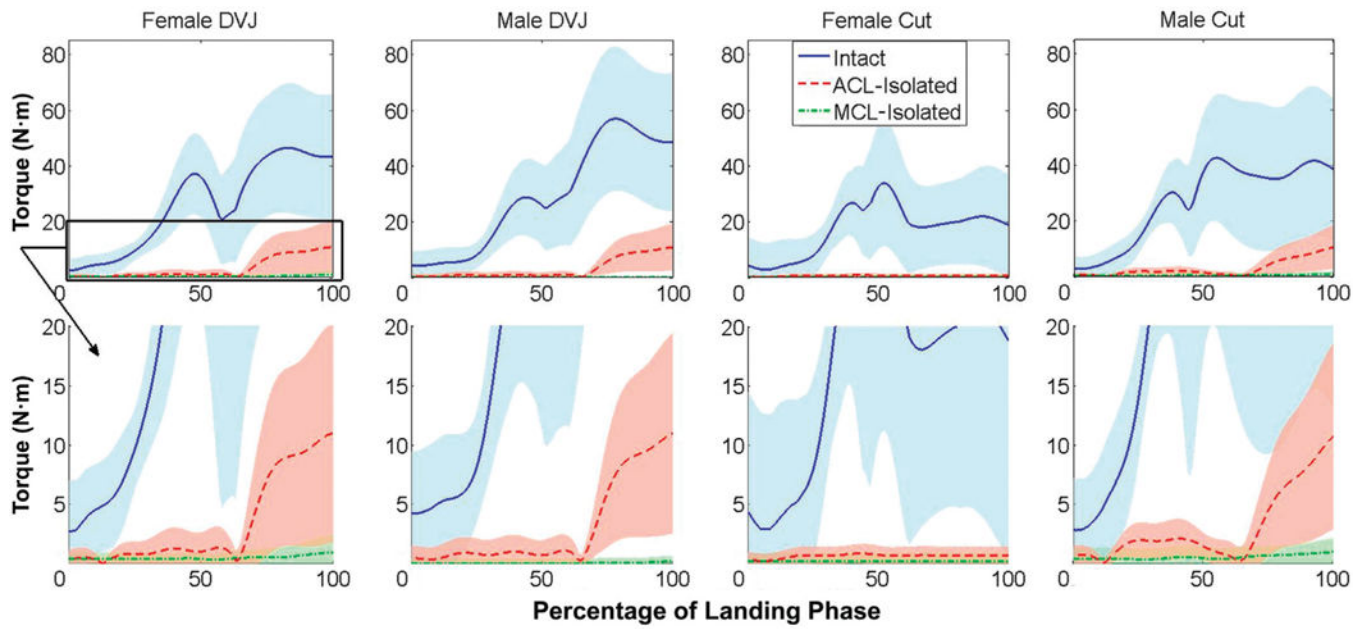


**Figure 7.**

Total knee torque during landing phase of athletic tasks. Sum of the average rotational components during each simulated task for the intact knee, anterior cruciate ligament (ACL)-isolated knee, and medial collateral ligament (MCL)-isolated knee. As seen in the translational components, the ACL had greater overall torsional contributions to knee joint restraint than the MCL. DVJ, drop vertical jump.

**TABLE 1**Peak Forces and Torques Generated During Simulations Performed in the ACL-Isolated Condition<sup>a</sup>

	Female DVJ	Male DVJ	Female Cut	Male Cut
Force, %BW				
Posterior	0.2	0.2	0.2	0.0
Anterior	-4.6 <sup>b</sup>	-5.0 <sup>b</sup>	-0.1	-4.9 <sup>b</sup>
Lateral	0.1	0.1	0.1	0.0 <sup>b</sup>
Medial	-1.8 <sup>b</sup>	-1.5 <sup>b</sup>	-0.1	-2.0 <sup>b</sup>
Distraction	2.9	2.9	0.1	2.7
Compression	-0.1	-0.2	-0.3 <sup>b</sup>	-0.1
Torque, Nm				
External	0.1	0.1	0.0	0.1
Internal	-0.2	-0.1	0.0	-0.1
Extension	0.9	0.8	0.6 <sup>b</sup>	1.5 <sup>b</sup>
Flexion	-8.2 <sup>b</sup>	-8.6 <sup>b</sup>	0.1	-8.0 <sup>b</sup>
Abduction	2.9	2.4 <sup>b</sup>	-0.1	3.1 <sup>b</sup>
Adduction	-0.5 <sup>b</sup>	-0.4 <sup>b</sup>	-0.3	-0.7

<sup>a</sup>Forces and torques values are directional: that is, opposing forces along a single axis generated opposite signs. The posterior, lateral, distraction, external, extension, and abduction directions are represented by positive values. ACL, anterior cruciate ligament; BW, body weight; DVJ, drop vertical jump.

<sup>b</sup>Significant difference between anterior cruciate ligament and medial collateral ligament.

TABLE 2

Peak Forces and Torques Generated During Simulations Performed in the MCL-Isolated Condition<sup>a</sup>

	Female DVJ	Male DVJ	Female Cut	Male Cut
Force, %BW				
Posterior	0.2	0.1	0.1	0.3
Anterior	-0.4 <sup>b</sup>	-0.1 <sup>b</sup>	-0.1	-0.2 <sup>b</sup>
Lateral	0.6	0.2	0.0	0.5 <sup>b</sup>
Medial	-0.1 <sup>b</sup>	-0.1 <sup>b</sup>	-0.1	-0.1
Distraction	3.0	0.9	0.4	2.9
Compression	-0.1	0.0	0.1 <sup>b</sup>	0.0
Torque, N m				
External	0.1	0.1	0.0	0.1
Internal	-0.1	0.0	0.0	0.0
Extension	0.2	0.1	0.1 <sup>b</sup>	-0.3 <sup>b</sup>
Flexion	-0.5 <sup>b</sup>	-0.2 <sup>b</sup>	0.0	-0.9 <sup>b</sup>
Abduction	0.6 <sup>b</sup>	0.1 <sup>b</sup>	-0.2	0.2 <sup>b</sup>
Adduction	0.1 <sup>b</sup>	-0.1 <sup>b</sup>	-0.3	-0.3

<sup>a</sup>Forces and torques are again directional. Posterior, lateral, distraction, external, extension, and abduction are represented by positive values. BW, body weight; DVJ, drop vertical jump; MCL, medial collateral ligament.

<sup>b</sup>Significant difference between anterior cruciate ligament and medial collateral ligament.